Reference Microphones Selection for Feedforward Active Noise Control Exploiting Microphone Networks

1st Yanrong He
College of Computer Science
Inner Mongolia University
Hohhot, China
yrhe@mail.imu.edu.cn

2nd De Hu*
College of Computer Science
Inner Mongolia University
Hohhot, China
cshood@imu.edu.cn

***Abstract*—Recent advances in feedforward active noise control (ANC) often require a reference microphone (RM) near each potential noise source to capture "clean" noise. However, in practice, the position of some noise sources is unavailable and may change with time, resulting in poor ANC performance. To overcome this shortcoming, a novel ANC system based on microphone networks is designed which allows for higher spatial resolution and thus captures high-quality recordings. Instead of using the entire microphone network, we select the most contributive subnetwork to act as the RMs in the ANC system to reduce the computational load of ANC tasks. Here, the best subnetwork is determined by minimizing the output noise power via Boolean programming. Experimental results show that the performance of the proposed method is close to the optimal performance using exhaustive searching.**

***Index Terms*—active noise control, feedforward control, convex optimization, microphone networks.**

I. Introduction

Active noise control (ANC) has attracted extensive attention in various applications, including headphones [1], headrests [2], vehicles [3], to name a few. In the traditional single-channel feedforward ANC system [4], a reference microphone (RM) is adopted to capture noise information. Then, the ANC controller emits "antinoise" by a secondary source to cancel the noise at the control point. Usually, it requires a fixed RM near the noise source to capture "clean noise" [5]. However, in practice, some noise sources are inaccessible and their positions may change over time, leading to low-quality noise recordings as well as poor ANC performance.

To obtain high-quality recordings, the multichannel feedforward ANC system was proposed, which employs multiple RMs to sample the sound field [6]. Specifically, Shi *et al.* proposed a 4-channel ANC system and validated its advantage on ANC windows [7]. Subsequently, Shen *et al.* demonstrated that the use of multiple RMs tends to increase the reference-to-interference ratio, which in turn improves the ANC performance [8]. Theoretically, the more RMs, the better the ANC performance. However, using all RMs may lead to an excessive computational burden, which affects the real-time processing requirement. To this end, it is vital to select an informative subset of RMs.

Recently, some RMs selection methods were developed to determine the most informative RM subset for ANC systems [9]–[11]. Iwai *et al.* selected those RMs that satisfy the causality relative to the error microphone, and the causality is determined by the time difference of arrival (TDOA) estimate between the RM and the error microphone [9]. Instead, Zhang *et al.* analyzed the coherence between the received signals of the RM and the error microphone, then concluded that the RM with a higher coherence coefficient makes a greater contribution to the multichannel feedforward ANC system [10]. Based on this basis, Shen *et al.* proposed a coherence-based RMs selection algorithm, which puts RMs with lower coherence coefficients to sleep [11]. However, since the above criteria do not directly reflect noise reduction performance, it is questionable whether using them is beneficial in multichannel feedforward ANC systems.

In this paper, instead of arranging RMs in advance, we use the microphone network to capture noise information. Due to the ad hoc nature, the microphone network has a higher spatial resolution [12], thus providing high-quality "clean noise". In order to reduce computational complexity, selecting the best subnetwork from the microphone network (to act as the RMs) is important, especially for a large-scale microphone network. To this end, we develop a novel RMs selection algorithm, in which the best subset of RMs is determined by minimizing the output noise power at the control point via Boolean programming. In doing so, the proposed method can obtain near-optimal RMs, which outperform the existing RMs selection strategies.

II. Fundamentals

A. Multichannel Feedforward ANC System

Let us consider a typical multichannel feedforward ANC system (Fig. 1), where the ANC controller receives the acoustic noises captured by I RMs and then emits the "antinoise" by a secondary source to cancel the noise at the control point

*: Corresponding Author. This work was supported by the National Natural Science Foundation of China under Grants 62361045 and 62201297.

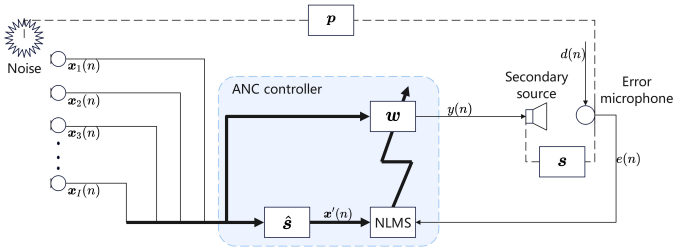

Fig. 1. Block diagram of the multichannel feedforward ANC system.

(error microphone position). The control signal $y(n)$ generated at time n can be represented by

$$y(n) = \sum_{i=1}^{I} \boldsymbol{x}_i^{\mathrm{T}}(n)\boldsymbol{w}_i, \tag{1}$$

where superscript $(\cdot)^{\mathrm{T}}$ indicates the transpose, $\boldsymbol{x}_i(n) = [x_i(n), x_i(n-1), ..., x_i(n-M+1)]^{\mathrm{T}}$ with $x_i(n)$ denoting the received signal of the ith RM at time n, and $\boldsymbol{w}_i$ is the M-order control filter corresponding to RM i.

The error microphone is placed at the desired control point to monitor the residual noise signal $e(n)$, which can be expressed as

$$e(n) = d(n) - y(n) * s(n), \tag{2}$$

where '$*$' denotes linear convolution, $d(n)$ represents unwanted noise through the primary path $\boldsymbol{p}$ (with $\boldsymbol{p}$ being the path between the noise source and the error microphone), and $s(n)$ is the impulse response of the secondary path $\boldsymbol{s}$ between the secondary source and the error microphone. During the system working, $d(n)$ can be estimated by

$$\hat{d}(n) = e(n) + y(n) * \hat{s}(n), \tag{3}$$

where $\hat{d}(n)$ is the estimate of $d(n)$, and $\hat{s}(n)$ is the estimate of $s(n)$, which can be obtained through offline modeling [13].

The objective of the multichannel feedforward ANC system is to minimize $e(n)$ through optimizing the filter coefficient $\boldsymbol{w} = \left[\boldsymbol{w}_1^{\mathrm{T}}, \boldsymbol{w}_2^{\mathrm{T}}, \cdots, \boldsymbol{w}_I^{\mathrm{T}}\right]^{\mathrm{T}}$, i.e.,

$$\min_{\boldsymbol{w}} \quad \mathbb{E}\left\{e^2(n)\right\}, \tag{4}$$

where $\mathbb{E}\{\cdot\}$ denotes the mathematical expectation. For real-time processing, the multiple reference filtered-x normalized least mean square (MRFxNLMS) algorithm [14] replaces $\mathbb{E}\left\{e(n)^2\right\}$ in (4) with its instantaneous form $e^2(n)$, obtaining the following recursive solution

$$\boldsymbol{w}_i(n+1) = \boldsymbol{w}_i(n) + \frac{\mu}{\beta + \sum_{i=1}^{I}\|\boldsymbol{x}_i'(n)\|^2}\boldsymbol{x}_i'(n)e(n), \tag{5}$$

where $\boldsymbol{w}_i(n)$ is the update of $\boldsymbol{w}_i$ at time n, μ is the step-size parameter, $\|\cdot\|$ represents the l_2 norm, β is the regularization parameter. $\boldsymbol{x}_i'(n) = [x_i'(n), x_i'(n-1), ..., x_i'(n-M+1)]^{\mathrm{T}}$ with $x_i'(n) = x_i(n) * \hat{s}(n)$.

Such a multichannel feedforward ANC system assumes that the RMs are placed near the potential noise sources before the ANC procedure [5]. However, the position of all the noise sources is not available in advance. Some noises are unpredictable, and their positions may change over time. Once it appears, the arranged RMs are difficult to capture "clean" noises, resulting in poor noise reduction performance.

B. ANC Exploiting Microphone Networks

Thanks to the scalability and versatility, microphone networks [12] offer a higher spatial resolution than the traditional single microphone (or the microphone array), as the number and position of the microphones are no longer fixed. In such a configuration, there is a higher probability that at least one microphone node is near each potential noise source, capturing high-quality recordings for multichannel feedforward ANC systems. Still, using the entire network to perform MRFxNLMS filtering may introduce a large computational load, affecting real-time processing. To this end, it is essential to select an informative subnetwork.

C. RMs Selection

RMs selection is often performed from a small number of noisy observations by activating all RMs (Fig. 2). During this period, all observations can be fed to the ANC controller to execute noise cancellation. Once the RMs selection is complete, only the selected RMs are reserved while other RMs are put to sleep. If a change in the sound field is detected, all RMs are reactivated to repeat the above RMs-selecting operation.

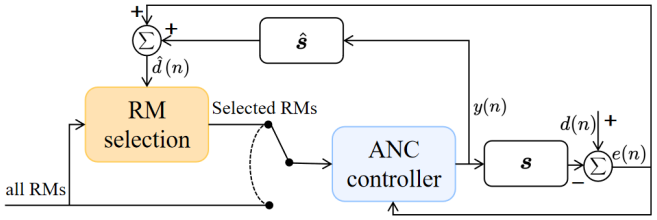

Fig. 2. Signal processing flow, where the internal structure of the ANC controller is shown in Fig. 1.

In [15], Hase *et al.* proposed an RMs selection approach based on the causality constraint. Specifically, the ith RM satisfies the causality constraint if and only if

$$\mathrm{TDOA}(\boldsymbol{x}_i, \hat{\boldsymbol{d}}) > D_C + D_s, \tag{6}$$

where $\hat{\boldsymbol{d}} = [\hat{d}(1), \hat{d}(2), ..., \hat{d}(N)]^{\mathrm{T}}$ is the desired signal of length N, $\boldsymbol{x}_i = [x_i(1), x_i(2), ..., x_i(N)]^{\mathrm{T}}$ is the received signal of RM i, and $\mathrm{TDOA}(\boldsymbol{x}_i, \hat{\boldsymbol{d}})$ is the TDOA from the noise source to the error microphone and RM i, D_C is the computational delay of the ANC controller, and D_s is the delay of the secondary path. Based on the above, the RMs that satisfy the constraint (6) are selected to perform the MRFxNLMS filter.

By doing so, the computational complexity of the multichannel feedforward ANC system can be reduced if some RMs do not meet (6). However, when many RMs satisfy the causality constraint, the computational load is still heavy. In other words, we can not specify the number of activated RMs by (6). Furthermore, it is questionable whether the causality constraint is actually optimal for noise reduction. These two issues are addressed in the next section through the development of a novel RMs selection method.

III. Reference Microphones Selection for Feedforward ANC in Microphone Networks

In order to obtain the best subset of RMs (or nodes) from a given microphone network, we minimize the residual noise power after constraining the number of activated nodes. Such a criterion is more intuitive than the causality constraint rule in (6), as the residual noise power directly reflects the ANC performance.

Exactly as in the study [15], here we conduct the RMs selection from the received signals of length N. In this case, problem (4) is equivalent to

$$\min_{\boldsymbol{w}} \quad \underbrace{(\hat{\boldsymbol{d}}-\boldsymbol{X}\boldsymbol{w})^{\mathrm{T}}}_{\boldsymbol{e}^{\mathrm{T}}}\underbrace{(\hat{\boldsymbol{d}}-\boldsymbol{X}\boldsymbol{w})}_{\boldsymbol{e}}, \tag{7}$$

where $\boldsymbol{e}=[e(1),e(2),...,e(N)]^{\mathrm{T}}$, $\boldsymbol{X}=\begin{bmatrix}\boldsymbol{X}_1 & \boldsymbol{X}_2 & \cdots & \boldsymbol{X}_I\end{bmatrix}$ with $\boldsymbol{X}_i=\begin{bmatrix}\boldsymbol{x}_i'(1) & \boldsymbol{x}_i'(2) & \cdots & \boldsymbol{x}_i'(N)\end{bmatrix}^{\mathrm{T}}$. Then, the closed-form solution of (7) is given by

$$\hat{\boldsymbol{w}}=(\boldsymbol{X}^{\mathrm{T}}\boldsymbol{X})^{-1}\boldsymbol{X}^{\mathrm{T}}\hat{\boldsymbol{d}}. \tag{8}$$

A. RMs Selection Model

A Boolean selection vector is first introduced as

$$\boldsymbol{v}=[v_1,v_2,\ldots,v_I]^{\mathrm{T}}\in\{0,1\}^I, \tag{9}$$

where $v_i=1$ indicates that node i is selected and vice versa. In addition, we use I_v to specify the number of selected RMs. Using a sensor selection matrix $\boldsymbol{\Phi}_v$, the selected microphone recordings $\boldsymbol{X}_v$ can be expressed by a submatrix of $\boldsymbol{X}$, i.e.,

$$\boldsymbol{X}_v=\boldsymbol{X}\boldsymbol{\Phi}_v^{\mathrm{T}}, \tag{10}$$

where $\boldsymbol{\Phi}_v\in\{0,1\}^{(I_vM)\times(IM)}$ is a submatrix of $\boldsymbol{V}=\mathrm{diag}(\boldsymbol{v})\otimes\mathbf{I}_M$ after all-zero rows (corresponding to the unselected sensors) have been removed, $\mathrm{diag}(\boldsymbol{v})$ denotes a diagonal matrix with $\boldsymbol{v}$ on its diagonal, and symbol '$\otimes$' denotes the Kronecker product while $\mathbf{I}_M$ represents an M-order identity matrix. It is evident that $\boldsymbol{\Phi}_v$ has the following characteristics

$$\boldsymbol{\Phi}_v\boldsymbol{\Phi}_v^{\mathrm{T}}=\mathbf{I}_{I_vM},\quad \boldsymbol{\Phi}_v^{\mathrm{T}}\boldsymbol{\Phi}_v=\boldsymbol{V}, \tag{11}$$

where $\mathbf{I}_{I_vM}$ is an (I_vM)-order identity matrix. After substituting $\boldsymbol{X}$ in (8) with $\boldsymbol{X}_v$, the optimal filter coefficient for a subset of I_v nodes determined by $\boldsymbol{v}$ will be

$$\hat{\boldsymbol{w}}_v=(\boldsymbol{X}_v^{\mathrm{T}}\boldsymbol{X}_v)^{-1}\boldsymbol{X}_v^{\mathrm{T}}\hat{\boldsymbol{d}}. \tag{12}$$

B. Loss Function Construction

Combining (12) and (7), the residual noise signal $\boldsymbol{e}_v$ using the selected nodes can be expressed as

$$\boldsymbol{e}_v=\hat{\boldsymbol{d}}-\boldsymbol{X}_v(\boldsymbol{X}_v^{\mathrm{T}}\boldsymbol{X}_v)^{-1}\boldsymbol{X}_v^{\mathrm{T}}\hat{\boldsymbol{d}}. \tag{13}$$

Then, $\boldsymbol{v}$ is determined by minimizing the output noise power, yielding

$$\begin{aligned}\min_{\boldsymbol{v}}\quad & \boldsymbol{e}_v^{\mathrm{T}}\boldsymbol{e}_v\\ \text{s.t.}\quad & \mathbf{1}^{\mathrm{T}}\boldsymbol{v}=I_v,\ \boldsymbol{v}\in\{0,1\}^I,\end{aligned} \tag{14}$$

where $\mathbf{1}$ represents the vector with all elements being 1. The problem (14) is non-convex due to the selection matrix $\boldsymbol{\Phi}_v$ and the Boolean variable $\boldsymbol{v}$. To this end, we relax this problem to a convex one in the next subsection.

C. Convex Relaxation

The output noise power in problem (14) can be derived as

$$\begin{aligned}\boldsymbol{e}_v^{\mathrm{T}}\boldsymbol{e}_v&=\hat{\boldsymbol{d}}^{\mathrm{T}}(\mathbf{I}_L-\boldsymbol{X}\boldsymbol{\Phi}_v^{\mathrm{T}}(\boldsymbol{\Phi}_v\boldsymbol{X}^{\mathrm{T}}\boldsymbol{X}\boldsymbol{\Phi}_v^{\mathrm{T}})^{-1}\boldsymbol{\Phi}_v\boldsymbol{X}^{\mathrm{T}})\hat{\boldsymbol{d}},\\&=\hat{\boldsymbol{d}}^{\mathrm{T}}\hat{\boldsymbol{d}}-\hat{\boldsymbol{d}}^{\mathrm{T}}\boldsymbol{X}\underbrace{\boldsymbol{\Phi}_v^{\mathrm{T}}(\boldsymbol{\Phi}_v\boldsymbol{X}^{\mathrm{T}}\boldsymbol{X}\boldsymbol{\Phi}_v^{\mathrm{T}})^{-1}\boldsymbol{\Phi}_v}_{\boldsymbol{Q}_v}\boldsymbol{X}^{\mathrm{T}}\hat{\boldsymbol{d}}.\end{aligned} \tag{15}$$

In order to avoid the non-linearity within $\boldsymbol{\Phi}_v\boldsymbol{X}^{\mathrm{T}}\boldsymbol{X}\boldsymbol{\Phi}_v$, the matrix $\boldsymbol{X}^{\mathrm{T}}\boldsymbol{X}$ is decomposed as

$$\boldsymbol{X}^{\mathrm{T}}\boldsymbol{X}=\lambda\mathbf{I}_{IM}+\boldsymbol{G}, \tag{16}$$

where λ is a positive constant and $\boldsymbol{G}$ is a positive semi-definite matrix. From (16), $\boldsymbol{Q}_v$ can be represented as $\boldsymbol{\Phi}_v^{\mathrm{T}}(\lambda\mathbf{I}_{I_vM}+\boldsymbol{\Phi}_v\boldsymbol{G}\boldsymbol{\Phi}_v^{\mathrm{T}})^{-1}\boldsymbol{\Phi}_v$. According to (11) and the matrix inversion lemma [16], $\boldsymbol{Q}_v$ can be further rewritten as

$$\boldsymbol{Q}_v=\boldsymbol{G}^{-1}-\boldsymbol{G}^{-1}(\boldsymbol{G}^{-1}+\lambda^{-1}\boldsymbol{V})^{-1}\boldsymbol{G}^{-1}. \tag{17}$$

Obviously, minimizing the output noise power in (15) is equivalent to maximizing its second term $\hat{\boldsymbol{d}}^{\mathrm{T}}\boldsymbol{X}\boldsymbol{Q}_v\boldsymbol{X}^{\mathrm{T}}\hat{\boldsymbol{d}}$. Therefore, problem (14) can be alternatively formulated as

$$\begin{aligned}\max_{\boldsymbol{v},\eta}\quad & \eta\\ \text{s.t.}\quad & \eta\le\hat{\boldsymbol{d}}^{\mathrm{T}}\boldsymbol{X}\boldsymbol{Q}_v\boldsymbol{X}^{\mathrm{T}}\hat{\boldsymbol{d}}\\ & \mathbf{1}^{\mathrm{T}}\boldsymbol{v}=I_v,\ \boldsymbol{v}\in\{0,1\}^I,\end{aligned} \tag{18}$$

where η is the lower bound of the term $\hat{\boldsymbol{d}}^{\mathrm{T}}\boldsymbol{X}\boldsymbol{Q}_v\boldsymbol{X}^{\mathrm{T}}\hat{\boldsymbol{d}}$. In addition, the first constraint in (18) can be reformulated via the linear matrix inequality [17] as

$$\begin{bmatrix}\boldsymbol{G}^{-1}+\lambda^{-1}\boldsymbol{V} & \boldsymbol{G}^{-1}\boldsymbol{c}\\ \boldsymbol{c}^{\mathrm{T}}\boldsymbol{G}^{-1} & \boldsymbol{c}^{\mathrm{T}}\boldsymbol{G}^{-1}\boldsymbol{c}-\eta\end{bmatrix}\succeq\boldsymbol{O}_{IM+1}, \tag{19}$$

where $\boldsymbol{c}=\boldsymbol{X}^{\mathrm{T}}\hat{\boldsymbol{d}}$. Afterward, we relax $v_i\in\{0,1\}^I$ to $0\le v_i\le 1$, and transform (18) into a convex programming

$$\begin{aligned}\max_{\boldsymbol{v},\eta}\quad & \eta\\ \text{s.t.}\quad & (19)\\ & \mathbf{1}^{\mathrm{T}}\boldsymbol{v}=I_v,\ 0\le v_i\le 1,\end{aligned} \tag{20}$$

which can be solved by existing solvers such as CVX [18] or SeDuMi [19]. Note that the nodes with the indices of the largest I_v elements in $\boldsymbol{v}$ are activated to perform MRFxNLMS filtering. By doing so, the computational complexity can be reduced significantly while maintaining good noise reduction performance.

Remark I Mathematically, the convex relaxation in RMs selection, i.e., (15)-(20), shares similarities with the derivation in other sensor selection methods [20]–[22]. We would like to note that the difference between the proposed method and these methods includes the application scenario, the loss function, and the symbol definition. For example, [20] concerns a sensor selection problem in speech enhancement and the corresponding loss function is constructed by maximizing the output SNR.

IV. Simulation Result

In the following simulations, we assumed a noise environment similar to that inside a factory, as described in [9], where the control point remains stationary and the locations of the noise sources do not change frequently.

The simulation environment was an enclosure of size 3 m × 3 m, where $I = 20$ spatially distributed microphones were arranged to form a microphone network (Fig. 3). The three noise sources emitted the noise signal in turn. The sampling rate was 16kHz, the signal length for RMs selection was fixed to $N = 160000$ samples, and μ and β were set to 0.001 and 1.0×10^{-6}, respectively. In subsequent experiments, the normalized mean squared error (NMSE) in dB is used to evaluate noise reduction performance, which is given by

$$\text{NMSE} = 10\log_{10}\frac{\sum_{n=1}^{L} e^2(n)}{\sum_{n=1}^{L} \hat{d}^2(n)}, \tag{21}$$

where L represents the signal length for performing MR-FxNLMS filtering. In subsequent experiments, $L = 160000$ samples. In general, the lower the value of the NMSE, the better the noise reduction performance.

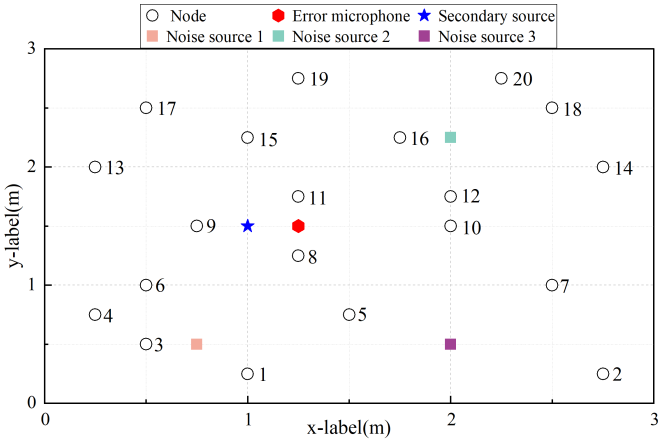

Fig. 3. Geometry configuration, including 1 loudspeaker, 1 error microphone, and 20 nodes in an enclosure.

A. Performance under different Filter Orders

In this experiment, we set $I_v = 1$, and the ANC performance was evaluated under different filter orders when activating only the 3rd noise source in Fig. 3.

From Table I, it can be seen that the optimal RM varies with increasing filter order, which provides the lowest NMSEs. This is because the increase of filter orders changes D_c in (6) and thus affects the optimal RM. Similarly, the RMs selected by the proposed method is also dependent on the filter order and is consistent with the optimal RM in most cases. (Although it does not find the optimal RM when $M = 30$, the NMSE of the proposed method is close to that of the optimal RM.) Note that the optimal solution can only be obtained from an NP-hard problem by exhaustive searching. The proposed method can get rid of the NP-hard problem, which runs more efficiently. In addition, state-of-the-art methods, including coherence-based selection (CBS) [11] and causality-constraint-based selection (CCS) [15], are independent of filter orders. The proposed method outperforms the above two methods, especially when the filter order is small.

TABLE I
NMSE and subset under different filter orders when $I_v = 1$.

	Filter order	15	20	25	30	35
Subset	Proposed	{5}	{6}	{6}	{3}	{3}
	Optimal	{5}	{6}	{6}	{6}	{3}
	CBS [11]	{9}	{9}	{9}	{9}	{9}
NMSE(dB)	Proposed	-19.16	-19.43	-19.51	-19.42	-19.59
	Optimal	-19.16	-19.43	-19.51	-19.50	-19.59
	CBS [11]	-6.94	-7.35	-7.44	-8.32	-9.15
	CCS [15]	-13.55	-15.10	-17.93	-19.40	-19.43

*Note: For the CCS method, we can not specify the number of RMs, and it always selects the subset {1,3,4,5,6} for all filter orders. Here, its NMSE was computed by averaging the NSMEs of all selected RMs.

B. Performance under Different Number of Activated RMs

In this experiment, the previous experimental settings were kept, but the filter order M was fixed at 20.

As shown in Fig. 4, the processing time per sample (PTPS) of the MRFxFLMS algorithm increases linearly as I_v increases. In addition, the proposed method provides the smallest NMSEs when selecting different numbers of RMs, especially when $I_v < 3$. If I_v is large, the NMSEs of all methods are comparable. That is, when selecting a small number of RMs to meet real-time requirements, the advantage of the proposed method is remarkable regarding noise reduction.

Although the running time for RMs selection (RTRMS) of the CCS method is the shortest, it is unable to specify the number of selected RMs, which is explicitly highlighted in Table I. Instead, it selects all nodes that satisfy (6). In contrast, the proposed method has an RTRMS that lies between the RTRMS of CCS and CBS algorithms, and it allows one to specify the number of selected RMs. As shown in Fig. 4, the proposed method achieves the lowest NMSE, which almost does not change when I_v increases from 1 to 5. The reason is that there is a large redundancy among the RMs. Our algorithm effectively finds and reduces this redundancy (by selecting $I_v = 1$ in this case), resulting in high computational efficiency.

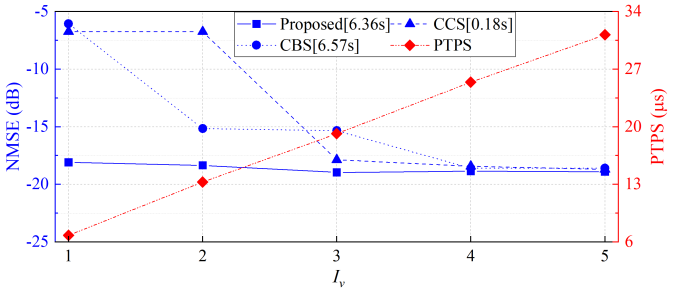

Fig. 4. NMSE, PTPS, and RTRMS under different I_v, where the value within [·] indicates the RTRMS.

C. Performance under Varying Noise environments

The ANC performance was tested in varying noise environments, with the three noise sources in Fig. 3 being activated sequentially. To reduce computational cost, we set $I_v = 1$ and

$M = 20$. Once the noise environment varies, the proposed method executes a reselection of RMs. In practice, the changes in the noise environment can be detected by monitoring the deterioration in noise reduction performance [9] (i.e., residual noise exceeding a specified threshold). During the RM reselection procedure, all RMs were activated to perform ANC until the new RM was available in the current noise environment. The averaged noise reduction (ANR), measured in dB, was used to evaluate the ANC performance under varying noise environments, which is calculated as

$$\mathrm{ANR(dB)} = 20\log_{10}(\frac{A_{e,n}}{A_{\hat{d},n}}), \tag{22}$$

where $A_{e,n} = \lambda A_{e,n-1} + (1-\lambda)\,|e(n)|$, $A_{\hat{d},n} = \lambda A_{\hat{d},n-1} + (1-\lambda)\left|\hat{d}(n)\right|$ with initial conditions $A_{e,0} = A_{\hat{d},0} = 0$, and $\lambda = 0.999$ is the forgetting factor.

As shown in Fig. 5, the selected RM varies with changing noise environments. In addition, when the noise environment changes, the ANR value slightly degrades during the first 16 s (including sampling time = 10 s and RTRMS = 6 s) where all RMs are activated. After the new RM is obtained and activated, the noise reduction effect is comparable to that of activating all RMs, demonstrating redundancy among RMs and highlighting the importance of RMs selection. The steady ANR is about -20 dB. This experiment further verifies the effectiveness of the proposed method in dynamic environments.

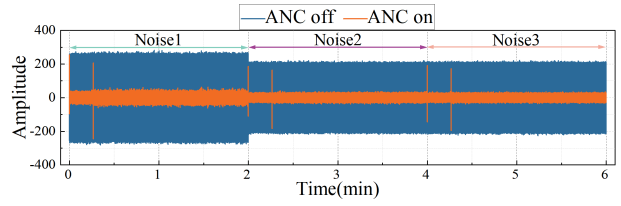

(a) Error signal

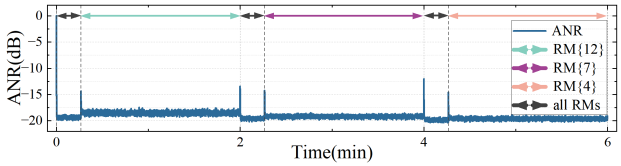

(b) ANR

Fig. 5. Noise reduction performance under changing noise environments.

V. Conclusion

This paper proposes an RMs selection method for multichannel feedforward ANC systems using microphone networks. We formulated the RMs selection problem by minimizing the output noise power using Boolean programming and solved it through convex optimization techniques. Numerical experiments confirmed that the proposed algorithm consistently selects the most contributing subset compared to the existing CBS and CCS methods. In our future work, we will investigate the RMs selection problem in multichannel feedforward ANC systems with multiple control points and multiple secondary sources.

References

[1] T. Watanabe, S. Kanai, and T. Atsumi, "Effects of wind noise on hybrid active noise cancellation headphones," in *Proc. IEEE Int. Conf. Ind. Technol.*, Orlando, FL, USA, 2023, pp. 1–6.

[2] S. Bagha, D. P. Das, and S. K. Behera, "Reference microphone free active headrest system for noise containing varying frequency tonal components," *IEEE Trans. Circuits Syst. II: Exp. Briefs*, pp. 3184 – 3188, Aug. 2023.

[3] S. Wang, H. Li, P. Zhang, J. Tao, H. Zou, and X. Qiu, "An experimental study on the upper limit frequency of global active noise control in car cabins," *Mech. Syst. Signal Process.*, vol. 201, p. 110672, Oct. 2023.

[4] S. M. Kuo and D. R. Morgan, "Active noise control: A tutorial review," *Proc. IEEE*, vol. 87, no. 6, pp. 943–973, Jun. 1999.

[5] X. Shen, D. Shi, and W.-S. Gan, "A hybrid approach to combine wireless and earcup microphones for ANC headphones with error separation module," in *Proc. Int. Conf. Acoust., Speech, Signal Process.*, Singapore, Singapore, 2022, pp. 8702–8706.

[6] T. Miyake, K. Iwai, and Y. Kajikawa, "Head-mounted multi-channel feedforward active noise control system for reducing noise arriving from various directions," *IEEE Access*, vol. 11, pp. 6935–6943, Jan. 2023.

[7] C. Shi, N. Jiang, H. Li, D. Shi, and W.-S. Gan, "On algorithms and implementations of a 4-channel active noise canceling window," in *Proc. Int. Symp. Intell. Signal Process. Commun. Syst.*, Xiamen, China, 2017, pp. 217–221.

[8] X. Shen, J. Ji, D. Shi, Z. Luo, and W.-S. Gan, "The principle underlying the wireless reference microphone enhancing noise reduction performance in multi-channel active noise control windows," *Mech. Syst. Signal Process.*, vol. 212, p. 111284, Apr. 2024.

[9] K. Iwai, S. Hase, and Y. Kajikawa, "Multichannel feedforward active noise control system with optimal reference microphone selector based on time difference of arrival," *Appl. Sci.*, vol. 8, no. 11, pp. 1–17, Nov. 2018.

[10] J. A. Zhang, N. Murata, Y. Maeno, P. N. Samarasinghe, T. D. Abhayapala, and Y. Mitsufuji, "Coherence-based performance analysis on noise reduction in multichannel active noise control systems," *J. Acoustical Soc. Amer.*, vol. 148, no. 3, pp. 1519–1528, Sep. 2020.

[11] X. Shen, D. Shi, and W.-S. Gan, "A wireless reference active noise control headphone using coherence based selection technique," in *Proc. Int. Conf. Acoust., Speech, Signal Process.*, Toronto, ON, Canada, 2021, pp. 7983–7987.

[12] M. Ferrer, M. de Diego, G. Piñero, and A. Gonzalez, "Affine projection algorithm over acoustic sensor networks for active noise control," *IEEE/ACM Trans. Audio, Speech, Lang. Process.*, vol. 29, pp. 448–461, Dec. 2020.

[13] L. J. Eriksson and M. C. Allie, "Use of random noise for on-line transducer modeling in an adaptive active attenuation system," *J. Acoustical Soc. Amer.*, vol. 85, no. 2, pp. 797–802, Feb. 1989.

[14] D. T. Slock, "On the convergence behavior of the LMS and the normalized LMS algorithms," *IEEE Trans. Signal Process.*, vol. 41, no. 9, pp. 2811–2825, Sep. 1993.

[15] S. Hase, Y. Kajikawa, L. Liu, and S. M. Kuo, "Multi-channel ANC system using optimized reference microphones based on time difference of arrival," in *Proc. IEEE 23rd Eur. Signal Process. Conf.*, Nice, France, 2015, pp. 305–309.

[16] K. B. Petersen and M. S. Pedersen, "The matrix cookbook," *Tech. Univ. Denmark*, vol. 7, Nov. 2008.

[17] S. P. Boyd and L. Vandenberghe, *Convex optimization*. Cambridge university press, 2004.

[18] M. Grant, S. Boyd, and Y. Ye, "CVX: Matlab software for disciplined convex programming," 2008.

[19] J. F. Sturm, "Using SeDuMi: A Matlab toolbox for optimization over symmetric cones," *Optim. Methods Softw.*, vol. 11, no. 1-4, pp. 625–653, Aug. 1999.

[20] J. Zhang, J. Du, and L.-R. Dai, "Sensor selection for relative acoustic transfer function steered linearly-constrained beamformers," *IEEE/ACM Trans. Audio, Speech, Lang. Process.*, vol. 29, pp. 1220–1232, Mar. 2021.

[21] S. P. Chepuri and G. Leus, "Sparse sensing for distributed detection," *IEEE Trans. Signal Process.*, vol. 64, no. 6, pp. 1446–1460, Mar. 2016.

[22] J. Zhang, S. P. Chepuri, R. C. Hendriks, and R. Heusdens, "Microphone subset selection for MVDR beamformer based noise reduction," *IEEE/ACM Trans. Audio, Speech, Lang. Process.*, vol. 26, no. 3, pp. 550–563, Dec. 2017.